

# THE KOLKHIDA SETUP UPGRADE

M.I. Tsulaya<sup>1</sup>, I.M. Salamatin, A.P. Sirotin, Yu.D. Mareev, T.L. Pikelner, D. Berikov

Joint Institute for Nuclear Research, 141980 Dubna, Moscow Region, Russia

<sup>1</sup> Andronikashvili Institute of Physics, Tbilisi, Georgia

The "Kolkhida" experimental setup designed for studies of neutron-optics phenomena in interactions of polarized neutrons with polarized nuclei has been constructed in JINR, at the IBR-2 pulsed reactor. In particular, we plan to study the nuclear precession of neutron spin in a wide range of neutron energies - from thermal to neutron resonance.

In the paper "Nuclear neutron precession" [1], which marked the beginning of a new research area – neutron optics of polarized media, it has been theoretically shown that the dependence of the refractive index of a neutron wave on mutual orientation of spins of the neutron and nucleus determines the neutron spin rotation around the direction of the target polarization. The precession frequency  $\omega$  depends on nuclear spin  $I$ , density of nuclei  $N$  and difference  $f^+ - f^-$  of amplitudes of neutron scattering by this nucleus corresponding to the states with total momentum of the neutron and nucleus  $I + \frac{1}{2}$ ,  $I - \frac{1}{2}$ :

$$\omega = \frac{4\pi N \hbar}{m_n} \frac{I}{2I+1} (f^+ - f^-) P_N,$$

where  $m_n$  is the neutron mass,  $P_N$  is the degree of nuclear polarization. The nuclear field, which causes the neutron spin precession, is generally called the effective magnetic field or pseudomagnetic field.

The projected studies on neutron nuclear precession will be performed in the neutron energy range from 0.062 eV to 2.3 eV.

The Kolkhida setup [2] consists for the following components:

- polarized neutron spectrometer;
- polarized nuclear target;
- control systems.

## Polarized neutron spectrometer

The spectrometer of polarized neutrons [2] is located at the tangential channel № 1 of the IBR-2 pulse reactor. A diagram of the spectrometer is shown in Fig. 1.

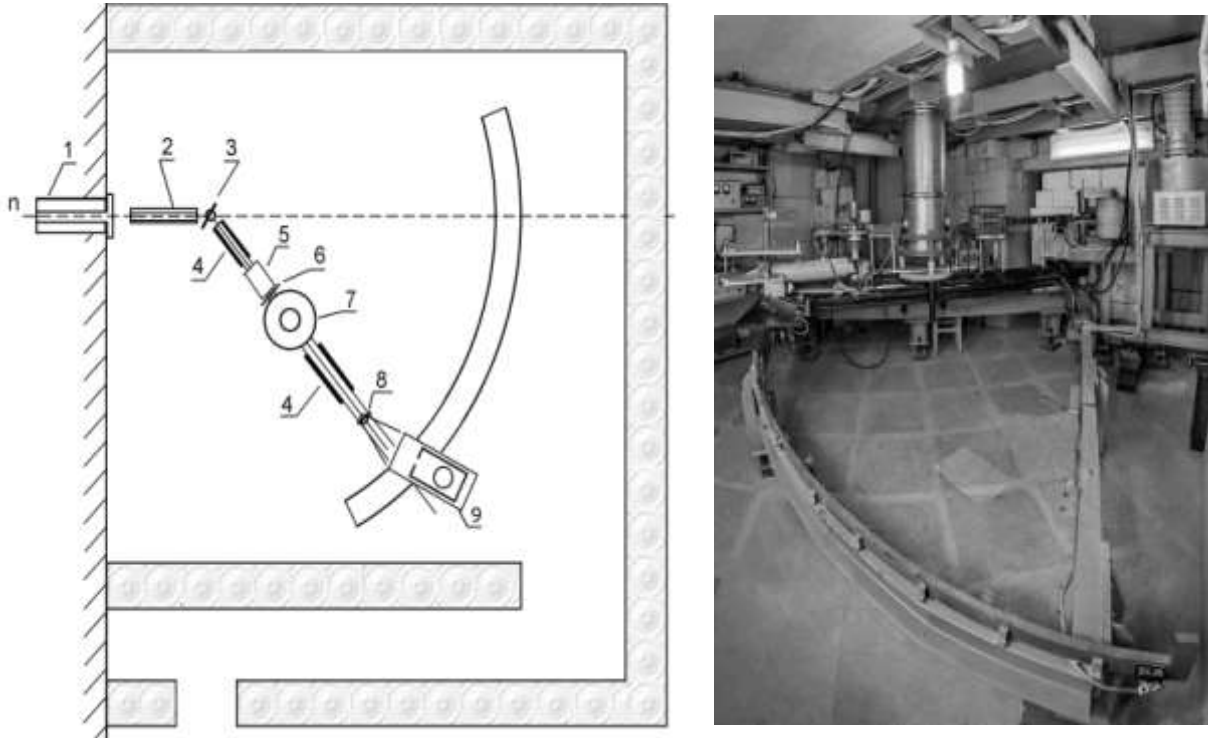


**Fig.1.** Diagram of the spectrometer:

1 – primary collimator; 2 – Soller collimator; 3 – polarizer crystal; 4 – guiding field electromagnets; 5 – Mezei flipper; 6 – shim; 7 – cryostat; 8 – analyzer crystal; 9 – detector.

The primary-neutron spectrum is formed in a moderator. The neutrons emerging from the moderator go through the biological shield by the channel with a primary collimator 1. Prior to entering the polarizer, the neutrons go through Soller collimator 2.

In order to polarize neutrons and to analyze their polarization we use Co-Fe single crystals.

A SNM-17 counter filled with  $^3\text{He}$  to a pressure of 10 atm is employed as a neutron detector. The detector entrance window has horizontal and vertical sizes of 10 and 50 mm. A  $^{235}\text{U}$  fission chamber with uranium layer thickness of  $100 \mu\text{g}/\text{cm}^2$  is used as a monitor.

The flight distance from the moderator in the reactor radiation zone to the detector is 15.9 m and comprises the following distances: moderator – polarizer, 12.4 m; polarizer – analyzer, 2.5 m; and analyzer – detector, 1.0 m.

The intensity and energy spectrum of the primary neutron beam incident on the polarizer were measured with the use of the RM-70 fission chamber. As a result, we obtained data on the neutron intensity and spectrum in an energy range of 10-200 meV. The chamber was placed at a flight distance of 13.5 m and the beam was limited by all of the above-mentioned collimators.

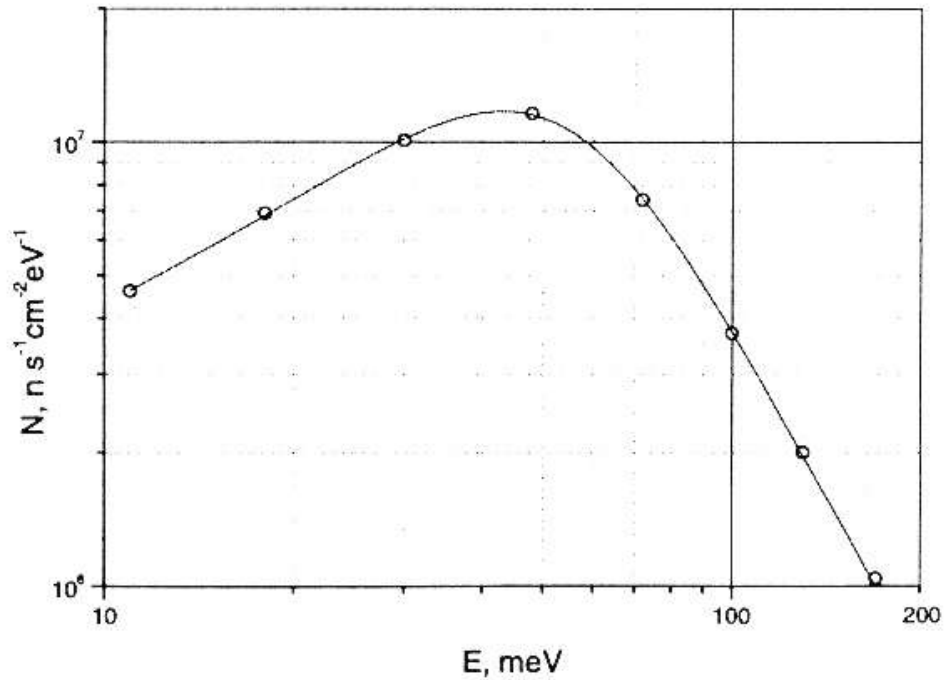


**Fig.2.** Energy distribution of the neutron flux incident upon the polarizer.

The neutron flux in the specified energy range was  $1.0 \times 10^6$  n/cm<sup>2</sup>s. Figure 2 shows the energy spectrum measured by the time-of-flight technique with the uranium fission chamber.

### Parameters of the polarized neutron beam

Angle $\theta$ (deg)	19	12	6	4	3
Wavelength $\lambda$ (Å)	1,15	0,74	0,37	0,25	0,19
Energy $E_n$ (eV)	0,062	0,15	0,60	1,3	2,3
Detector counting rate after the polarizer $n_1$ (s <sup>-1</sup> )	800	270	65	33	22
Polarized beam intensity $I_1$ (n/s cm <sup>2</sup> )	430	200	80	60	50
Detector counting rate after the analyzer $n_2$ (s <sup>-1</sup> )	70	23	3,1	0,6	0,2

For the Co-Fe single crystal, the neutron diffraction was measured in the Laue geometry for different angles  $\theta$  in a range of  $3^\circ - 19^\circ$  at which the incident neutrons hit the (200) surface. The measured values of the neutron wavelengths and energies for the listed angles  $\theta$  are presented in the table. The reflected beam maximum was determined by varying the  $\theta$  angle. The detector counting rate  $n_1$  and the intensity  $I_1$ , which takes into account the detector efficiency and the reflected beam area ( $s \cong 4\text{cm}^2$ ), are presented in the table.

Figure 3 shows time-of-flight spectra measured for  $\theta = 19^\circ$  (lower) and  $\theta = 6^\circ$  (upper). The time analyzer channel width was  $32 \mu\text{s}$ ,  $t$  – the channel number. Pointers 1-3 indicate the reactor burst position, the first-order diffraction peak, and the second-order reflection peak, respectively. The measurement time for each spectrum was 10 min. Because the instant counting rate was very high in the spectrum measurement for  $\theta = 19^\circ$ , the diffracted beam from the crystal-polarizer was filter-suppressed by a factor of ten. Figure 3 shows such a reduced peak. In the other measurements, suppression was not necessary.

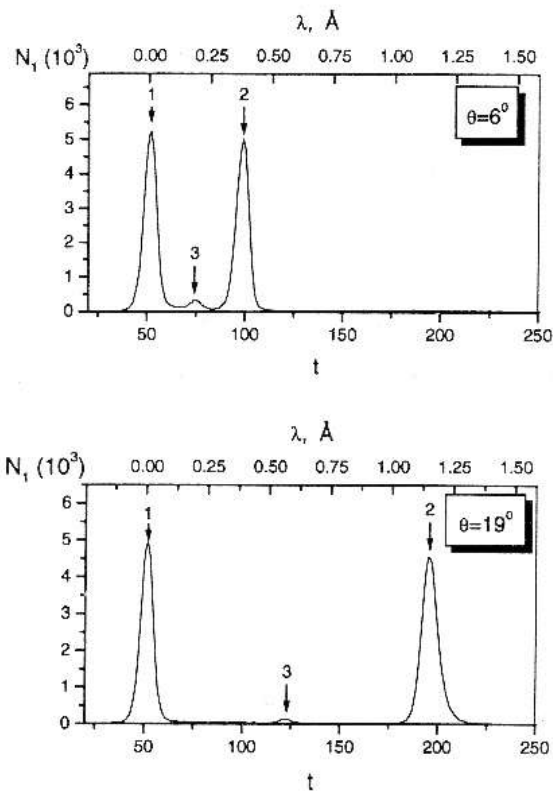


**Fig. 3.** Time-of-flight neutron spectra after the polarizer obtained for 10 min.

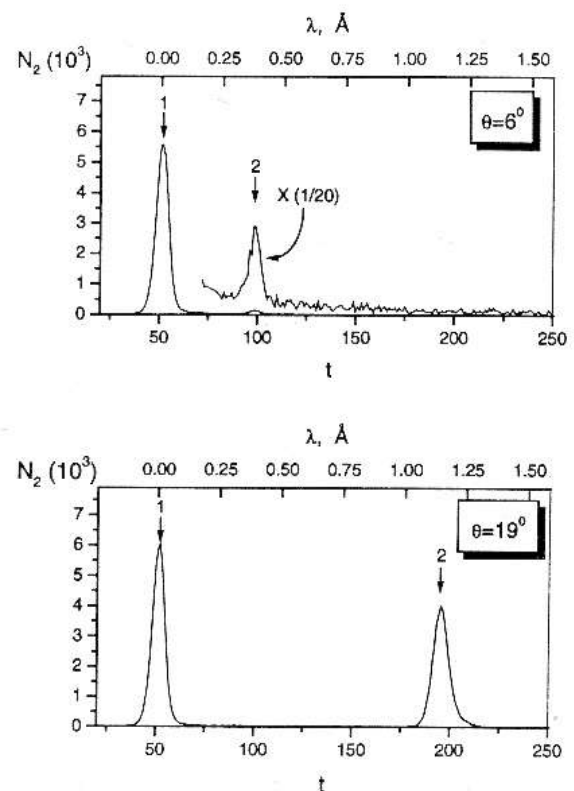


**Fig. 4.** Time-of-flight neutron spectra after the analyzer obtained for 10 min.

To obtain a beam of polarized neutrons and to analyze the polarization, a magnetic field was applied to the crystals, and the beam intensity reflected by the crystal-polarizer was measured. Time-of-flight spectra for the same angles  $\theta = 19^\circ$  and  $6^\circ$  after reflection from the crystal-analyzer are shown in Fig. 4, and values of the

detector counting rate  $N_2$  after reflection from the second crystal are presented in the table.

The polarization measured in different runs was spread between  $P = 0.9$  and  $P = 0.98$ , depending on the beam collimation in the guiding magnetic fields. The polarization was measured for  $\theta$  angles ranging from  $19^\circ$  to  $3^\circ$ , which corresponded to neutron energies from 0.062 to 2.3 eV, and was within this range for all energies.

### **Polarized nuclear target**

At the Kolkhida setup a “brute force” method will be used to polarize nuclei – when the nuclear target is deeply cooled in a constant, strong magnetic field [2].

For the polarized nuclear target a  $^3\text{He}$ - $^4\text{He}$  refrigerator has been constructed. It consists of the following components:

- $^4\text{He}$  cryostat
- $^3\text{He}$  circulation system and  $^3\text{He}$  in  $^4\text{He}$  dilution stages
- Superconducting solenoid

### **$^4\text{He}$ cryostat**

The helium cryostat (Fig.5) provides a temperature mode and vacuum for normal functioning of the  $^3\text{He}$ - $^4\text{He}$  refrigerator and superconducting solenoid.

**$^3\text{He}$  circulation system and  $^3\text{He}$  -  $^4\text{He}$  dilution stages.** The  $^3\text{He}$  circulation system is assembled on the basis of vacuum booster pump NVBM-2.5, vacuum rotary unit AVR-50 and leakproof mechanical pump NVG-2 connected in series (Fig.5). This pump group provides for  $^3\text{He}$  circulation rate  $\dot{n} = 1.07 \times 10^{-3}$  mole.

Gaseous  $^3\text{He}$  is supplied to the cryostat through two independent return lines I and II. Along the return lines,  $^3\text{He}$  passes through tubular heat exchangers, placed in the bottom parts of nitrogen bath 4 and helium baths 6 and 8. Upon condensation in tubular heat exchangers of bath 8,  $^3\text{He}$  passes through throttles  $D_1$  and  $D_2$  and then enters the heat exchanger located in the bottom part of evaporation bath (Fig. 5).

Upon leaving the evaporation bath heat exchanger,  $^3\text{He}$  is supplied to the system of continuous and discrete heat exchangers (Fig. 6).

The dilution bath is located in the effective volume of the superconducting solenoid. The dilution bath structure (Fig.7) can be easily disassembled. Dilution bath temperature is  $T=23$  mK at  $^3\text{He}$  circulation rate  $\dot{n} = 1.07 \cdot 10^{-3}$  mole/s.

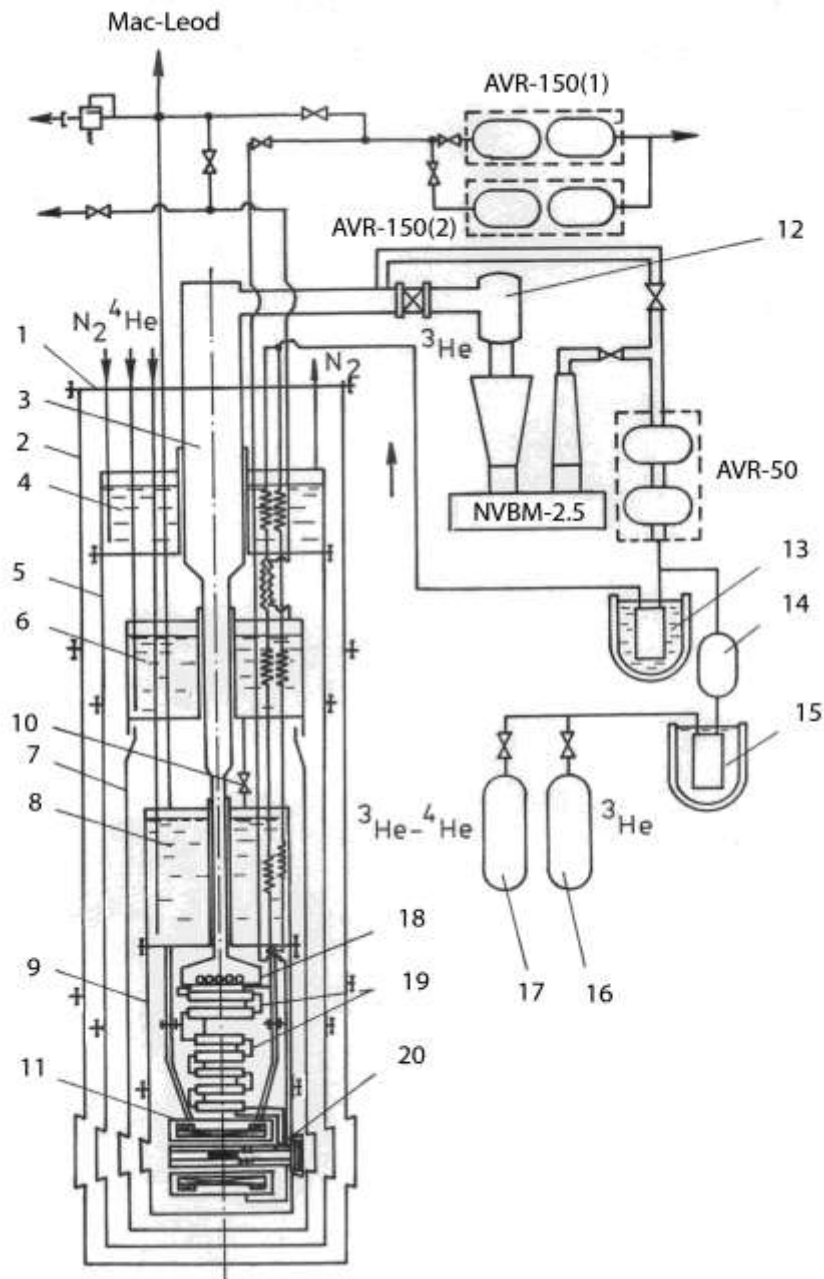


**Fig.5.**  $^3\text{He} - ^4\text{He}$  dilution cryostat diagram with a superconducting solenoid.

1 - main flange; 2 - vacuum housing; 3 - central  $^3\text{He}$  pump-out pipe; 4 - nitrogen bath; 5 - nitrogen screen; 6 - helium bath; 7 - helium screen; 8 - helium bath to be evacuated; 9 - dilution stage helium screen; 10 - cryo-valve; 11 - superconducting solenoid; 12 - nitrogen trap of booster pump NVBM-2.5; 13 - oil filter; 14 - pump NVG-2; 15 - carbon trap; 16 -  $^3\text{He}$  storage cylinder; 17 -  $^3\text{He} - ^4\text{He}$  mixture storage cylinder; 18 - evaporation bath; 19 - heat exchangers; 20 - dilution bath.

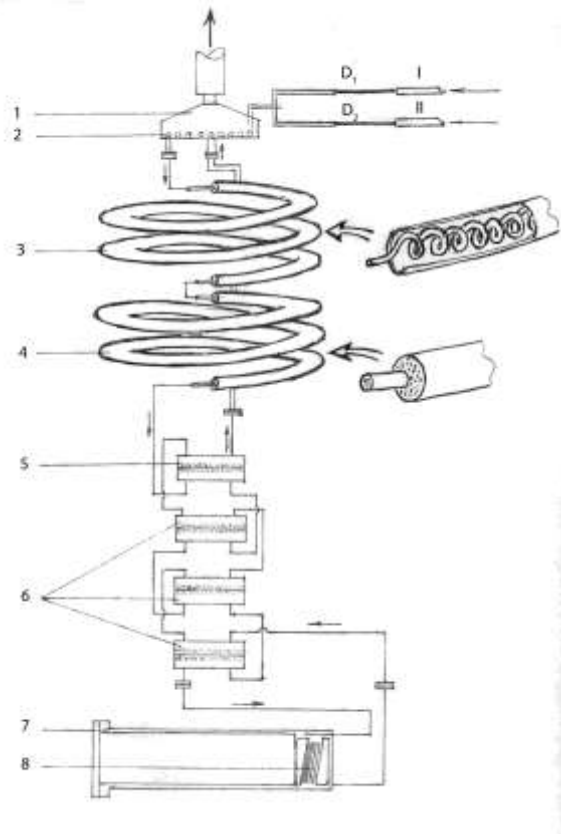


**Fig. 6.** Diagram (a) and general view (b) of  $^3\text{He} - ^4\text{He}$  dilution stages.

1 – evaporation bath; 2 – evaporation bath heat exchanger; 3 – continuous tubular heat exchanger; 4 – continuous sintered heat exchanger; 5 – discrete copper heat exchanger; 6 – discrete heat exchangers from sintered silver powder; 7 – dilution bath; 8 – ferromagnetic neutron resonator with polarized nuclear target.

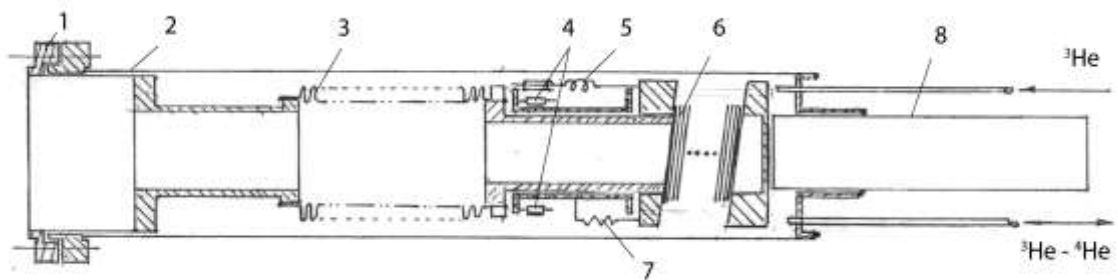


**Fig. 7.** Dilution bath.

1 – plug; 2 – housing; 3 – bellows; 4 – temperature sensors; 5 – NMR-resonator; 6 – ferromagnetic neutron resonator with a sample; 7 – heater; 8 – centering plug-tube.

## **The Kolkhida setup upgrade**

We upgraded (it was upgraded) electronics for the Kolkhida setup executive mechanisms' control system in time with the start of the modernized pulse reactor IBR-2M. In particular, for the polarized neutron spectrometer we have chosen the step engines FL57STH76-1006B for changing angular positions of the shoulder, the detector platform, the polarizer and the analyzer, while for detecting rotation angles we have chosen OCD-SL00B-0016-C100-CRW sensors. We have a computer-controlled system for rotations of various components of the setup. It uses an algorithm, which implements selection of gaps. The angles are set with the precision of  $<0.1$ deg (the resolution of sensors is 0.0055deg).

Besides the aforementioned devices, the computer also controls the precise source of current. It allows us to set the current in the superconducting magnet on up to 110A with the precision of 5mA, which is required for investigation of the nuclear precession of the neutron spin.

We have also upgraded the polarized nuclear target:

- We have updated the cryostat service infrastructure by replacing old vacuum devices with modern ones.
- We have created a new, modern dilution bath for the cryostat.
- We have created a new cryostat component for neutron investigation of specimens in strong magnetic fields at room temperature.

## **Software**

The software consists of an experiment automation system (EAS) and a group of programs for the experimental setup adjustment.

The existence of the neutron and nuclear polarization equipment – which is part of the Kolkhida setup – gives us a flexibility to choose from wide range of problems and research methods. The number of specimen conditions control devices is expected to grow and this puts specific requirements on the software architecture, which should flexibly adapt to the changes in experimental methods and at the same time allow to reuse already developed programs. According to the principles described in the paper [3] we have developed a component system with service-oriented structure. The components of this system depend neither on the experimental methodology nor on the construction of the spectrometer. They are built in executable format and their descriptions are stored in a database. The user describes methodology of a concrete experiment with the help of an universal dialogue application, which does not depend on the spectrometer construction and which uses component descriptions stored in the database. The EAS is assembled automatically in accordance with the current description of the experiment methodology. A specialized distributed software environment – which uses dynamic “remote linking” method – allows different components to interact with each other.

There are two groups of components within EAS: basic components, which allow execution of main tasks (specimen conditions control, data registration and archiving), and helper components (data visualization, express data analysis etc). For the basic components we implemented a “rigid” interaction logic, which guarantees the delivery of messages to the client. On the other hand, it is not

considered an error if a client ignores message generated by some of helper components.

We have developed the following basic components:

- User interface
- Main control program
- DAQ-subsystem
- Component for controlling the engines
- Component for controlling the angular sensors
- Component for controlling the precise source of current
- Component for controlling the pulse-width modulation
- Component for controlling the spin-flipper and the following helper components:
  - Data visualization program
  - Express data analysis program etc.

The EAS architecture and its working principles allow us to extend the number of the basic components and to develop new helper components without changing the already developed code. The users can exploit the system and extend its functionality with new components (provided such components already exist) without a help from software developers.

### **Conclusion**

We have completed the upgrade of the Kolkhida experimental setup. During the upgrade process we developed the new Experiment Automation System, which allows significant lowering of costs for the future software development. The system has been implemented with the use of modern software technologies, it allows reusing already existing applications and it is reliable and easy to use.

### **References**

- [1] V.G. Barishevski, M.I. Podgorecki, Zh. Eksp. Teor. Fiz., 47, 1964, 3(9), p.1050, Sov. Phys. JETP, 20, 1965, p.704.
- [2] Y.G. Abov, M.I. Tsulaia, V.P. Alfimenkov, L.Lason, et al., NIM, A, v.601,i.3, 4, 2009, p.317.
- [3] V.N. Shvetsov, I.M. Salamatin, K.M. Salamatin, Preprint, to be printed, Dubna 2013.